

# LiCellMo™

Product in Development



## ***LiCellMo — Paving the Way for Metabolic Research and Cell & Gene Therapy\****

***Live cell metabolic analysis paves the way not only  
for metabolic research, but also the manufacturing  
of significant CGT products.***

*The investigation and understanding of cellular metabolism has become increasingly important in recent years. In the expanding fields of cancer immunotherapy, stem cell research, and commercial biological manufacturing process development, greater metabolic control is resulting in more effective outcomes and higher quality end products. In the field of cancer immunotherapy — such as CAR-T and TCR-T therapy, stem cell research including embryonic stem (ES) and induced pluripotent stem (iPS) cells and commercial cell and gene therapy (CGT) manufacturing process development — all require investigating and understanding the metabolic activities of cells which are critical.*

Learn more: <https://www.phcbi.com/us/biomedical/live-cell-metabolic-analyzer>

\* Product not yet commercially available

**phcbi**

# Insights into product and process related challenges of lentiviral vector bioprocessing

Christopher Perry<sup>1,2,3</sup> | Noor Mujahid<sup>1</sup> | Yasu Takeuchi<sup>2,3</sup> | Andrea C. M. E. Rayat<sup>1</sup> 

<sup>1</sup>Department of Biochemical Engineering, University College London, London, UK

<sup>2</sup>Division of Infection and Immunology, University College London, London, UK

<sup>3</sup>Biotherapeutics and Advanced Therapies, Scientific Research and Innovation, Medicines and Healthcare Products Regulatory Agency, South Mimms, Potters Bar, UK

## Correspondence

Andrea C. M. E. Rayat, Department of Biochemical Engineering, University College London, Bernard Katz Bldg, Gower St, London WC1E 6BT, UK.

Email: [andrea.rayat@ucl.ac.uk](mailto:andrea.rayat@ucl.ac.uk)

## Present address

Christopher Perry, Rentschler ATMP Ltd., Sycamore House, 2 Gunnels Wood Rd, Stevenage, SG1 2BP, UK.

## Funding information

UKRI Engineering and Physical Sciences Research Council; Centre for Doctoral Training at the Department of Biochemical Engineering, Grant/Award Number: EP/L01520X/1; Doctoral Training Partnership at UCL, Grant/Award Numbers: EP/N509577/1, EP/T517793/1; National Institute for Biological Standards and Control (NIBSC)—Medicines and Healthcare Products Regulatory Agency (MHRA)

## Abstract

Lentiviral vectors (LVs) are used in advanced therapies to transduce recipient cells for long term gene expression for therapeutic benefit. The vector is commonly pseudotyped with alternative viral envelope proteins to improve tropism and is selected for enhanced functional titers. However, their impact on manufacturing and the success of individual bioprocessing unit operations is seldom demonstrated. To the best of our knowledge, this is the first study on the processability of different Lentiviral vector pseudotypes. In this work, we compared three envelope proteins commonly pseudotyped with LVs across manufacturing conditions such as temperature and pump flow and across steps common to downstream processing. We have shown impact of filter membrane chemistry on vector recoveries with differing envelopes during clarification and observed complete vector robustness in high shear manufacturing environments using ultra scale-down technologies. The impact of shear during membrane filtration in a tangential flow filtration-mimic showed the benefit of employing higher shear rates, than currently used in LV production, to increase vector recovery. Likewise, optimized anion exchange chromatography purification in monolith format was determined. The results contradict a common perception that lentiviral vectors are susceptible to shear or high salt concentration (up to 1.7 M). This highlights the prospects of improving LV recovery by evaluating manufacturing conditions that contribute to vector losses for specific production systems.

## KEYWORDS

bioprocess, envelope proteins, lentiviral vector, pseudotype, scale-down, vector stability

## 1 | INTRODUCTION

Lentiviral vectors (LVs) are commonly used to deliver and stably integrate genetic information to recipient cell chromosomes for the treatment of numerous disorders. Their usage as therapy agents is

increasing up to 33% of all gene transfer vectors and up to 66% of all *ex vivo* gene transfers within clinical trials in the UK (CGT Catapult, 2022). There are three approved therapies using LVs covering both gene and cell therapy applications (United States of America FDA, 2022), with many more candidates advancing past

Christopher Perry and Noor Mujahid should be considered as joint first authors of equal contribution.

This is an open access article under the terms of the Creative Commons Attribution License, which permits use, distribution and reproduction in any medium, provided the original work is properly cited.

© 2023 The Authors. *Biotechnology and Bioengineering* published by Wiley Periodicals LLC.

Phase I/II. However, the current bottleneck of high cost and complexity of manufacturing has led to some of these candidates not being advanced to market, thus limiting patient access to these potential therapies (Fox et al., 2023).

### 1.1 | Lentiviral vectors: Basics

LVs are enveloped vectors derived from lentiviruses, commonly HIV-1 (Durand & Cimarelli, 2011). They have a transgene holding capacity of approximately 8 kilobases (kb) (Chen et al., 2018), with rare neutralizing antibodies against them (Kalidasan et al., 2021), and have been made safe to minimize risks (Milone & O'Doherty, 2018) which makes them superior to other vectors. LVs are commonly manufactured using the transient transfection system where genetic information required to form LV is split across several plasmids and transfected into a cell line with the aid of a transfection reagent. There are four generations of lentiviral vector system; with the second and third generations being the more common systems used in both academic and clinical laboratories, with the third and fourth generation more seen in labs for clinical applications (Kalidasan et al., 2021; Milone & O'Doherty, 2018). The first generation LVs are now seldom used due to safety concerns while fourth generation LVs, which are relatively new, are not yet widely available (Kalidasan et al., 2021). Third-generation lentiviral vector system require four plasmids: two of these are packaging plasmids encoding *gag* and *pol* (*gag-pol*) and the other encoding *rev*. The other two encodes for the envelope protein and the transgene (i.e., gene of interest). For the second generation lentiviral vector system, the packaging vector are all combined in a single plasmid, hence this system requires only three plasmids to produce functional LVs (Perry & Rayat, 2021). The three-plasmid system is typically used in industry and academia for fundamental work. It has a lower burden of production (i.e., fewer plasmids needed). The four-plasmid system is often preferred due to improved clinical safety and is generally used in industry. Lentiviral vectors are also pseudotyped with envelope proteins from other viruses. HIV-1's primary tropism is confined to CD4+ cells (Dalglish et al., 1984). This innate restriction necessitates the encapsulation with alternative envelope proteins to target broader ranges of cells of clinical importance. Stable vector producer cell lines, in contrast to the transient system, have all genetic information for vector production integrated into their chromosomes and may produce all vector components for longer periods which benefits clinical applications (Comisel et al., 2021; Perry & Rayat, 2021; Sakuma et al., 2012).

### 1.2 | Envelope proteins

LVs pseudotyped with different envelope proteins can provide better stability or withstand the rigorous manufacturing process (Cronin et al., 2005). Due to their presence at the vector surface, they interact directly with the bulk media and therefore experience varieties of physicochemical conditions throughout downstream

processing (DSP) such as varying shear forces, salt concentrations and pH conditions. They additionally interact directly with physical media such as filters and chromatography base matrices. The historical envelope protein of choice is vesicular stomatitis virus glycoprotein (VSV-G) based on its broad tropism and high gene-transfer efficiency as well as robustness in lab scale purification techniques such as ultracentrifugation (Kim & Lim, 2017; Naldini et al., 1996). However, VSV-G is not a panacea for envelope protein applications; for example, during LV generation, cytotoxicity and syncytia formation are apparent (Burns et al., 1993; Hoffmann et al., 2010).

Of particular interest are envelope proteins originating from within the vesiculovirus family, notably Cocal-G. Sharing 72% homology with VSV-G (Munis et al., 2018), Cocal-G enveloped LVs can possibly share its broad tropism while decreasing cellular cytotoxicity (Humbert et al., 2016). Additionally, another envelope of interest is derived from the RD114 envelope, which originates from a feline endogenous retrovirus and is better suited to transducing CD34+ cells and haematopoietic stem cells, with some CAR-T applications (Ghani et al., 2009; Müller et al., 2020) while showing stability like VSV-G (Dautzenberg et al., 2021). Cocal-G and RD114 derived vectors are also of interest to manufacturing due to their offering of stable producer cells for vector generation which may provide an alternative modality that reduces plasmid and transfection reagent consumption and variability (Humbert et al., 2016; Sanber et al., 2015). Both of these envelope proteins are not inactivated by complement (Humbert et al., 2016; Takeuchi et al., 1994) which may provide beneficial applications compared to VSV-G.

### 1.3 | Challenges in LV manufacture

Different avenues of LV manufacturing platform are covered in our review (Perry & Rayat, 2021). A typical LV manufacturing route is described in Figure 1a: note the multiple membrane processes (i.e., clarification, concentration/diafiltration and sterile filtration) often utilized alongside chromatography as the main purification step. Due to their lipid enveloped structure, the stability of LVs is thought to be influenced by temperature, freeze-thaw, ionic strength, adsorption, pH and shear stress experienced during the manufacturing steps. The mechanism of LV loss through these stressors is yet to be fully investigated (Moreira et al., 2020). Although some stability studies have been performed in the past (e.g., Dautzenberg et al., 2021; Tijani et al., 2018), these have focused on chemical and thermal stability rather than on the individual unit operations and their interaction. In the field of recombinant protein production, including macromolecular therapies, understanding the interactions between the product and the unit operations has led to improvement of yields, reduction in cost and development of a robust purification strategy (Huisman et al., 2000; Zydney, 2021). The systematic study of LV manufacturing condition, the unit operations and their interactions (i.e., whole bioprocess analysis) is currently a gap in vector manufacturing. The low recovery and loss of vector functionality,

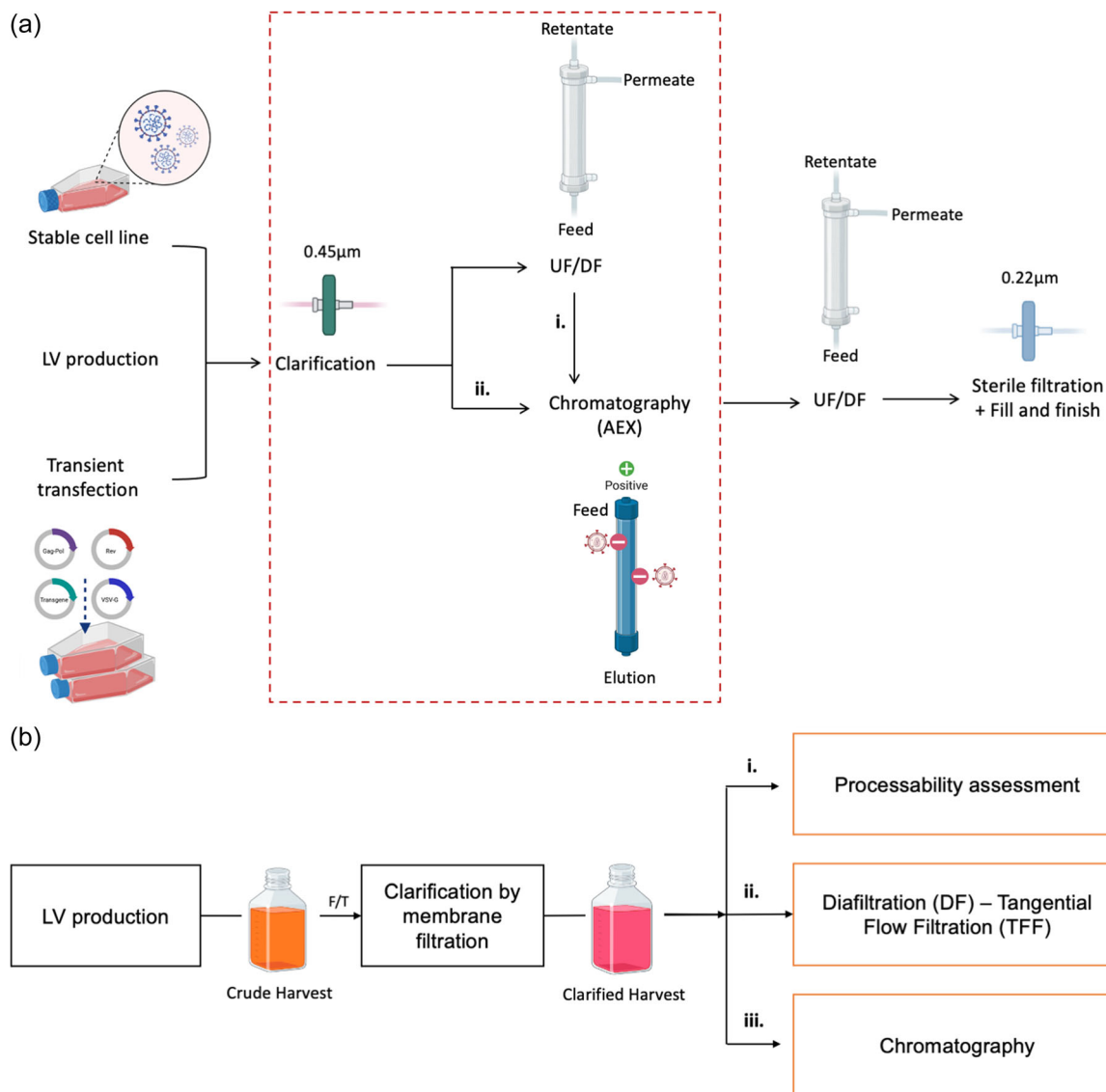


**FIGURE 1** Manufacturing considerations for lentiviral vector (LV) products: (a) Options for process sequence showing (i) a step for tangential flow ultrafiltration (UF) to concentrate the vectors and/or for buffer exchange or diafiltration (DF) to aid the subsequent anion exchange chromatography (AEX) and (ii) a simplified process option where there is no UF/DF before AEX; (b) studies to evaluate the (i) manufacturability or processability of vectors and the conditions that may affect, (ii) diafiltration, or (iii) chromatography steps. Elements of the image were created with BioRender.com. F/T, freeze-thaw.

as well as the differences in quality requirements (i.e., purity and potency) for in vivo and ex vivo applications are key challenges in LV production (McCarron et al., 2016). The latter requires product and process review on a case-by-case basis (McCarron et al., 2016) while the former (i.e., LV losses) can be addressed by rational bioprocess development for the fundamental study and understanding of LV bioprocessing (Perry & Rayat, 2021). Bioprocess investigations at the earliest opportunity during product development would enable the design and creation of robust LVs for manufacture.

In this regard, scale-down bioprocess models mimicking manufacturing operations and high throughput studies could prove beneficial. These models can provide crucial process information while balancing the need for experimentation with reduced resource

requirements, often in 10 s of milliliters. Ultra scale-down (USD) modeling is such an approach, where complex interactions can be decoupled and studied under varied process conditions (e.g., TMP, shear, flow rate) with the aim of understanding a pilot scale run and offering ways of improvement (Titchener-Hooker et al., 2008). The various USD models have been developed to simulate normal flow and tangential flow filtration (TFF), depth filtration, and continuous flow centrifugation (Rayat et al., 2016). Recently, a USD membrane shear device (Fernandez-Cerezo et al., 2019) was developed to mimic the shear encountered at the surface of membranes during TFF operations. This device aided the prediction of membrane process performance of monoclonal antibodies during TFF (Fernandez-Cerezo et al., 2020). Other USD models have also been used in conjunction

with computational modeling which facilitated the identification of better process results (Nunes et al., 2023).

## 1.4 | Aims

This work studies lentiviral vector recovery and determines the impact of different aspects of manufacturing on the vector to improve LV bioprocessing, including the choice of envelope protein. The objectives were to investigate the effect of process shear, manufacturing duration and temperature, and pump flow on LV recovery; the impact of membrane materials; the impact of chromatography buffers on LVs; and to demonstrate an optimized chromatography operation. These insights can benefit manufacturers of LV and provide awareness on the impact of envelope protein choice on vector bioprocessing. Additionally, bioprocess studies were made using three-plasmid and four-plasmid vector systems (i.e., second and third generation LVs). The focus is on the bioprocess characterization, mainly the recovery of infectious particles, of these different LV systems and pseudotypes using the ultra scale-down methodologies. The mechanistic understanding of the differences in enveloped proteins (e.g., biophysical characterization) is not part of the scope of this paper, although it is recognized that this would have some relevance and that the materials generated at scale-down may enable such studies. To the best of our knowledge, this is the first

study that investigates and compares the processability of different preparations of pseudotyped LVs.

## 2 | MATERIALS AND METHODS

### 2.1 | Materials

HEK293T cells were obtained from American Type Culture Collection (ATCC RL-11268). Cell culture reagents (Dulbecco's modified Eagle medium [DMEM] high glucose GlutaMAX, fetal bovine serum [FBS]), transfection complex media (Optimem), phosphate buffered saline (PBS), transfection reagent for the three-plasmid system, polyethylenimine (PEI), protein (Bradford) assay kit, DNA (Picogreen) assay kit are from Thermo Fisher Scientific. Viral RNA Kit was from Qiagen. The PEI used in the four-plasmid system is from Polyplus. Cell culture flask, T175 and Hyperflasks, are from Corning. Syringe filters, polyvinylidene difluoride (PVDF) and MCE 96-plate filters are from MilliporeSigma. Polyethersulfone (PES) and Nylon 96-plate filters are from Agilent, flat disc membranes from Thermo Fisher Scientific, Vivaspin filters from Sartorius, QA and DEAE 96-well CIM monoliths from BIA Separations (Ajdovščina, Slovenia). Buffers were prepared from stock buffers (1 M MOPS) and reagents (5 M NaCl, 10 M NaOH, 11.65 M HCl) from Thermo Fisher Scientific. Deionised water was from a Milli-Q system. Sources for plasmids used for LV production are listed in Table 1.

**TABLE 1** Cell culture and transient transfection conditions for lentiviral vector production.

Parameter	Values	
LV system	Three-plasmid system (3PS)	Four-plasmid system (4PS)
Vessel	Hyperflask (1720 cm <sup>2</sup> )	T175 (175 cm <sup>2</sup> ) (Batch 1 and 2) Hyperflask (1720 cm <sup>2</sup> ) Batch 3
Seeding density	1.45 × 10 <sup>5</sup> cells cm <sup>-2</sup>	75,000 cells cm <sup>-2</sup>
Envelope plasmids <sup>a</sup>	pRDproLF; or pMD2Cocal.G; or pMD.G	pRDproLF; or pMD2.CocalG; or pMD.G
GFP vector genome plasmid	GFP-BSR <sup>b</sup>	pRRLSIN.cPPT.PGK--GFP.WPRE <sup>c</sup>
HIV-1 protein plasmid(s)	p8.91 <sup>a</sup>	pRSV-Rev <sup>c</sup> ; and pMDLg/pRRE <sup>c</sup>
Plasmid ratio (by weight)	1:1:1.5 (env, p.891, genome)	3:2:4:1 (pMDLg/pRRE, pRSV-Rev, genome, env)
DNA (μg) per 1.0 × 10 <sup>6</sup> cells mL <sup>-1</sup>	2.06	1.5
DNA:PEI ratio (by weight)	1:3	1:1
Transfection reagent	PEI	PEI
Transfection complex media	Optimem	Optimem
DNA:PEI complex time	15 min	15 min

<sup>a</sup>Same plasmids as used in Tijani et al. (2018).

<sup>b</sup>Plasmids constructions were as described in Perry (2021).

<sup>c</sup>Plasmids were gifts from Didier Trono ([Addgene plasmid # 12252; <http://n2t.net/addgene:12252>; RRID:Addgene\_12252]; [Addgene plasmid # 12253; <http://n2t.net/addgene:12253>; RRID:Addgene\_12253]; [Addgene plasmid # 12251; <http://n2t.net/addgene:12251>; RRID:Addgene\_12251]) (Dull et al., 1998).

## 2.2 | LV production

The production of LV through transient transfection was performed with a three-plasmid system and a four-plasmid system. In brief, the HEK293T cells were seeded and grown in DMEM high glucose GlutaMAX supplemented with 10% FBS at 37°C and 5% CO<sub>2</sub>. After 24 h cells were transfected as per conditions listed in Table 1. Cells were exchanged into fresh media 24 h posttransfection while the conditioned media was discarded. The vector-containing medium was harvested at 48- and 72-h posttransfection in aliquots of 50 mL and stored at -80°C until required. At time of use, the vector was thawed for 30 min in a 37°C water bath.

To produce LVs from stable producer cell lines, WinPac-RDpro-GFP cells construction is as described in Sanber et al. (2015) and WinPac-Cocal-G-GFP cells construction is described in Perry (2021). Briefly, producer cells ( $3 \times 10^8$ ) were grown in Hyperflasks under antibiotics selection in 550 mL of complete media. Cells were exchanged into fresh media without antibiotics after 24 h. After a further 24 h, virus-containing media was harvested in aliquots of 50 mL and stored at -80°C until required at which point the vector was thawed in the same way as the transiently produced LVs.

## 2.3 | Processibility assessment

Thawed, crude LV harvest (100 mL each) was collected from stocks of four-plasmid transient LV production pseudotyped with VSV-G, RDpro and Cocal-G. These were clarified using 0.45 µm Millex HP PES syringe filters (4.5 cm<sup>2</sup>). A peristaltic pump (120U/DM2, Watson Marlow) with size 16 precision tubing (L/S<sup>®</sup>, Masterflex) pumped the LV material through to the filters at 5 mL min<sup>-1</sup> (30 RPM) using a PendoTech system. Samples were taken from the crude and clarified harvests for functional titer assay. To assess the impact of the very low shear pump on vector functionality, 10 mL of clarified harvest was pumped through the same set-up, this time with no filter attached. Additionally, 10 mL of clarified material were tested for manufacturing stability by placing the samples at ambient room temperature and at 4°C for 5 to 9 h which are typical duration in LV manufacturing.

## 2.4 | Clarification study

Each transiently generated three-plasmid LVs, pseudotyped with envelope protein VSV-G, RDpro and Cocal-G, (500 µL) was thawed, and applied in triplicate across 96-well 0.45 µm filter plates. Four membrane materials were tested, PES, PVDF, mixed cellulose esters (MCE), and nylon, representing commonly used membrane materials during clarification and bioburden reduction (Perry & Rayat, 2021). A TeVacS<sup>®</sup> system (Tecan) was used within a biosafety cabinet to apply 500 mbar vacuum and collect clarified filtrate.

## 2.5 | USD membrane shear study

An ultra scale-down membrane shear device was used as a TFF mimic (Fernandez-Cerezo et al., 2019). The device was loaded with a fresh membrane filter (25 mm diameter, PES 500 kDa). An Akta Pure (Cytiva) was used to transfer 20 mL of 0.1 M NaOH through the unit, incubated for 30 min while the permeate port is closed, before opening the port and flushing through 50 mL deionised water. A further 50 mL of DMEM was flushed through the unit. The unit was vented of any air and was kept full either with equilibrating media or sample until the end of any experiment.

The disc of the membrane device was rotated at either 0, 1000, 2000, 3000 or 4000 RPM which corresponds to estimated shear rates of 0, ~800, ~2000, ~4000, ~5500 s<sup>-1</sup>. To equilibrate the membrane, 18 mL of DMEM is flowed through the system at 1 mL min<sup>-1</sup>. Using an injection loop, 1 mL of vector-containing media (i.e., clarified harvest) was injected into device, followed by 8 mL of DMEM. From the point of injection, permeate was collected. At the end of the diafiltration, retentate was collected. Vectors were prepared as in Section 2.2. Before the membrane experiments, thawed vector-containing media was treated with 5 U mL<sup>-1</sup> final concentration of benzonase, incubated 1 h at room temperature before filtering with 0.45 µm filter. For control samples, vector was pumped through the unit without the rotating disc being turned-on and without any filter.

## 2.6 | USD shear study

A rotating disc shear device (kompAs<sup>®</sup>, UCL; Rayat et al., 2016) was used to apply shear forces to clarified vector harvests (0.45 µm PES syringe filter). The unit was filled with 20 mL of sample, then air bubbles removed before operating the disc at either 0, 3000, 6000, 9000, 12,000, 15,000, or 18,000 RPM for 20 s. For control, 20 mL sample was injected into the device and then immediately taken out. In this study, Cocal-G and RDpro LVs were from stable cell lines, while VSV-G was generated transiently. In another study, transiently produced four-plasmid system Cocal-G, RDpro and VSV-G LVs were used.

## 2.7 | Vector stability study

Frozen-thawed, transiently generated LV sample (20 mL) was concentrated 10× in Vivaspin 4 spin filters (100 kDa MWCO) which were previously washed with PBS (4000g for ~15 min). The concentrated vector was diluted 10x in the test buffers (Table 2), or PBS control. Additionally, buffers of increasing salt concentration were investigated (0–1.7 M NaCl in 20 mM MOPS, pH 7.4). Vector tubes were inverted several times before being left at room temperature for incubation. At 15-min intervals, 0.1 mL was removed and mixed 1:9 with warmed DMEM before being transferred to a plate for transduction assay.

**TABLE 2** Test buffers in vector stability study.

Monolith	LV pseudotype	Loading conditions of 20 mM MOPS buffer		Justification
		NaCl (M)	pH	
Condition 1	VSV-G	0.21	7.9	Optimal loading condition found for QA monolith
	Cocal-G	0.15	7.8	
	RDpro	0.22	7.9	
Condition 2	VSV-G	0.21	9.0	Optimal loading condition found for DEAE monolith
	Cocal-G	0.18	9.0	
	RDpro	0.24	9.0	

## 2.8 | Method for optimal chromatography

Transiently generated LVs (20 mL) were filtered (0.45 µm PES) and concentrated 10× in Vivaspin 20 (100 kDa MWCO). The concentrated vector was diluted 10× in 3 mL total volume of the loading buffer (either DMEM or 20 mM MOPS with different salt concentrations and pH). Specific loading conditions for the MOPS buffer are shown in Figure 8(iv) (R2). A 96-well monolith plate (0.2 mL QA) was placed on TeVacS deploying 500 mbar vacuum until the storage ethanol was removed. Ten column volumes of each of the following were dispensed in sequence between vacuum cycles: deionised water, 2 M NaCl solution, deionised water and binding buffer. The monolith wells were filled with 2 mL of sample vector. Flowthrough was collected. The wells were washed with additional 2 mL of binding buffer and collected, followed by elution buffer. All collected samples were immediately diluted 10× in PBS, before filtering through 0.45 µm sterile multiscreen filter plate. Functional titer was quantified by 72-h transduction assay, protein concentration by Bradford, and Picogreen assay for DNA. All samples were compared to the prechromatography sample (i.e., clarified harvest).

## 2.9 | Assays

### 2.9.1 | Functional titer assay

Functional titer (TU mL<sup>-1</sup>) was determined using the infectious titer assay described in Sanber et al. (2015) (48-h assay) and Ruscic et al. (2019) (72-h assay) where HEK293T cells were transduced with LV, and GFP expression measured using Flowcytometry (BD FacsCalibr or LSRFortessa, and then analyzed on FlowJo). The assay was performed in two formats (12- and 96-well). In the 12-well format, 3E+05 HEK293T cells in 300 µL were plated into a 12-well plate and transduced with 200 µL neat or diluted LV in the presence of 8 µg/mL of polybrene for a total volume of 500 µL. After 24 h, additional 1 mL of fresh media (DMEM and 10% FBS) was added. After another 48 h the samples were exposed to

trypsin, suspended, and fixed with 4% paraformaldehyde (PFA) and analyzed for GFP expression. This method was used for all samples apart from VSV-G (Batch 2 and 3), Cocal-G, RDpro in processability assessment. For the latter samples, the assay was scaled down 10× by volume from a 12-well plate format to a 96-well plate for high throughput testing. In both assay formats, each sample was prepared in triplicate wells and the titer for each well was calculated with %GFP of cell population between 1% and 20% using the following equation:

$$\text{Titre (TU mL}^{-1}\text{)} = \frac{\text{Number of cells at transduction} \times \frac{\% \text{GFP positive cells}}{100}}{\text{Vector input volume (mL)} \times \text{dilution factor}}$$

The average of the three wells are used as the sample titer and where there are biological repeats, the titers reported is the average of the sample titers. The percentage coefficient of variation (%CoV) of the triplicate transduction assay for a sample is usually <20%.

### 2.9.2 | RNA reverse-transcriptase polymerase chain reaction (RT-PCR)

The vector genome was isolated by QIAmp Viral RNA Kit (Qiagen), with lysis buffer containing carrier RNA and spiked with 2 ng Luciferase RNA (Promega). Vector absent samples (i.e., non-LV cell culture harvest) were used as negative control. The kit was used as per kit instructions.

### 2.9.3 | Total protein and double stranded DNA (dsDNA) assay

The total protein (Bradford assay kit) and dsDNA (Quant-it) were performed using kits as per manufacturers' instruction. Protein standard curve was generated using standard BSA (0.1–1.4 mg mL<sup>-1</sup>). Protein sample absorbance was measured using Tecan Infinite plate reader at 585 nm. For dsDNA measurement, control was generated using phage lambda DNA standard provided in the kit. Samples were read using Tecan Infinite plate reader and were excited at 485 nm and fluorescence measured at 520 nm.

## 2.10 | Data analysis

Data was analyzed and visualized using Prism version (GraphPad). "% Recovery" refer to the ratio of the amount of material in the main product stream of the unit operation to the amount in the feed × 100%. "(%Control)" refers to the amount of material after an experiment relative to the amount of the same material after a control experiment.

### 3 | RESULTS AND DISCUSSION

#### 3.1 | Processability assessment

The processability assessments (Figure 1b) were performed to investigate the stability of LVs as a result of going through unit operations (in this case, clarification step by membrane filtration) or being held at ambient or room temperature within expected durations of LV manufacturing. Clarification with 0.45  $\mu\text{m}$  PES syringe filter (Figure 2) showed a significant difference in functional

titers between crude harvest and clarified harvest ( $p=0.0078$ , Wilcoxon matched pairs signed rank test) across all batches of VSV-G, RDpro, Cocal-G. Additionally, the mechanical and temperature stability of LV was tested by applying very low shear using the peristaltic pump and keeping the material at 4°C and ambient temperature for the typical length of a manufacturing process (5–9 h). Statistical test of the clarified harvest compared to pump flow, ambient or 4°C showed no significant difference among these conditions for each pseudotyped LV. However, a weak correlation of lower functional titers appears with pump flow which needs

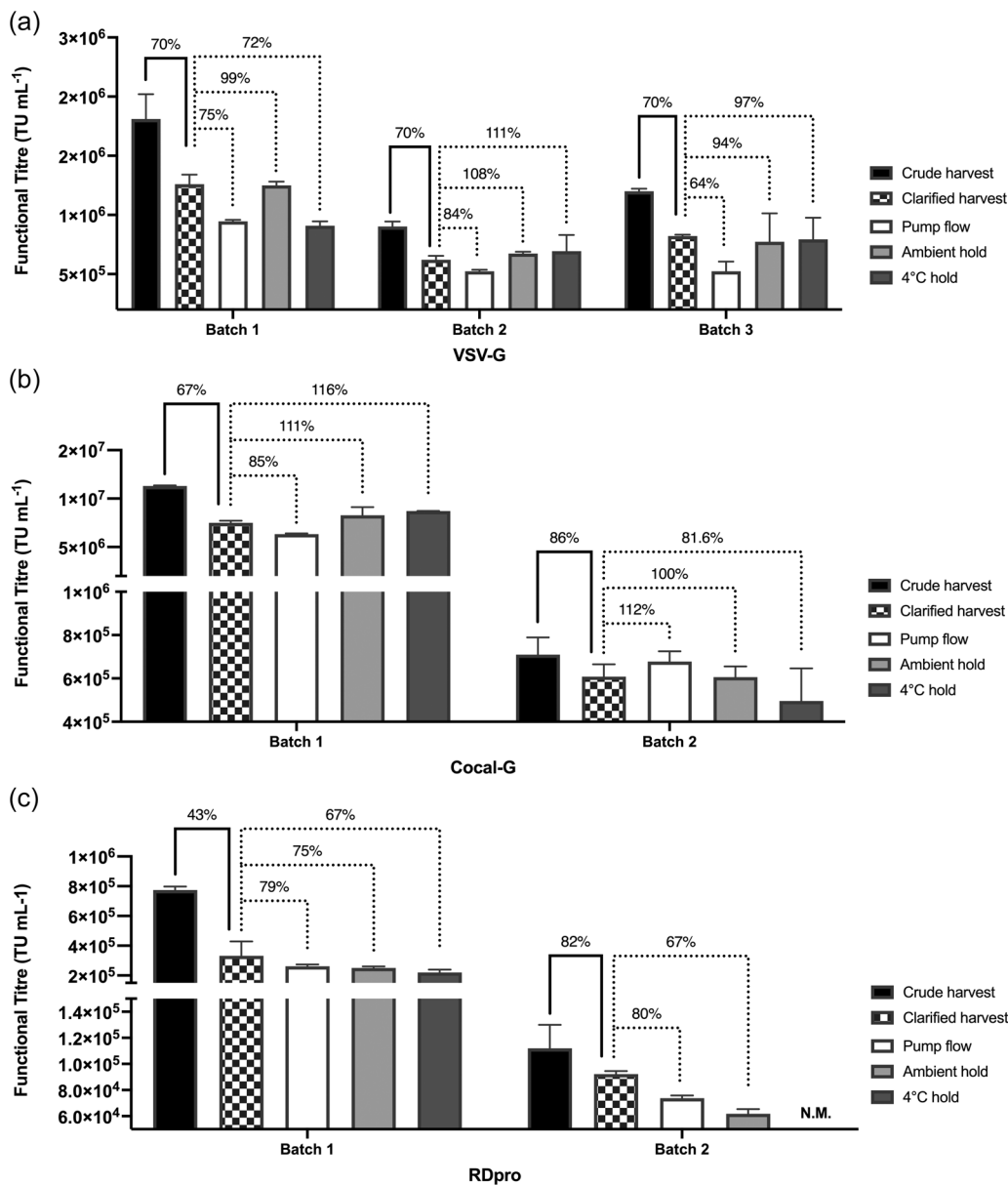


**FIGURE 2** Processability assessment of transiently produced four-plasmid pseudotyped lentiviral vector (LV) batches with envelope protein: (a) VSV-G, (b) Cocal-G, and (c) RDpro. Functional titers of harvest materials are shown before and after clarification by membrane filtration using 0.45  $\mu\text{m}$  Millex-HP PES filter (4.5  $\text{cm}^2$  filter area), controlled by PendoTech system and pumped through Watson Marlow 120U/DM2 using size 16 Masterflex® L/S® precision pump tubing at 5  $\text{mL min}^{-1}$  (30 RPM). The clarified harvest then underwent different processing conditions postclarification: flow through pump, ambient hold and 4°C hold at durations typical of overall manufacturing time. The %recovery between steps is noted on each bar. Error bars represent 1 SD based on  $N=3$  transduction assay technical repeats. N.M., not measured.



further investigation as the impact of the pump is combined with the impact of tubing material used. These results highlight that membrane filtration as a clarification step has the largest impact among the process conditions tested followed by the impact of pump which can indicate an effect of shear on LVs. The impact of pumps is relevant in all bioprocess steps and more so in concentration and diafiltration steps by TFF as the material recirculates through the pump and then an ultrafilter until the desired concentration and buffer exchange is achieved. The following sections further evaluate these: Section 3.2 on the impact of membrane types in clarification and Section 3.3 on the impact of shear during TFF operations.

### 3.2 | Clarification study

Clarification is used to remove cell and cellular debris from the crude supernatant and is often the initial step in the purification of lentiviral vectors. Recovery in this step using membrane clarification have been previously reported between 70% and 90% for VSV-G enveloped LVs, increasing to greater than 95% for physical particle recovery (Perry & Rayat, 2021). The types of membrane material used for clarification is varied in literature but there is limited, if not lacking, information on their process performance for LV recovery. Four common membrane materials were tested within this experiment at the same retention rating to determine membrane-specific effects on vector recovery. This initial work with LVs from the three-plasmid production system indicated that the choice of membrane material can have an impact on the recovery of LVs postclarification. It can be observed in Figure 3 that the PVDF membrane provided the higher recoveries for the specific LV feeds used in this work, while the PES

provided the lowest. This may be due to several factors. The geometry and the microstructures of the filters may better entrap vector particulates. While chemical interactions from the membrane's construction may have greater affinities to vectors with particular envelope proteins. The latter case may be why Cocal-G LVs report consistent lower recoveries (50%–85%) compared to RDPro and VSV-G pseudotyped LVs (80%–100%). Note that these LVs were from the three-plasmid system (i.e., second generation) and that the samples were treated with benzonase before clarification. In contrast to this, in Figure 2, the %functional vector recovery in clarified harvest using PES membrane range between 40% and 80% depending on the envelope protein; with Cocal-G and VSV-G LVs having the higher recoveries of 60%–80%. These LVs are from the four-plasmid system (i.e., third generation LVs) and were not treated with benzonase. These demonstrate that clarification of LVs from different plasmid-systems and with different pseudotypes do not consistently show the same recovery and therefore poses the need to be experimentally evaluated.

Also, there may be several types of membranes of the same base (e.g., PES-based membranes) in the market. It is worth investigating how these compare with each other. In an on-going study in our group, we are further investigating the nature of the membrane surfaces and their properties when exposed to LV products. This can elucidate the kind of interaction membrane materials have between vectors, their design, production platform, and formulation.

Other LV harvests may have a different result as different feeds (i.e., different plasmid system, cell lines, media, etc.) may have different interactions with the membranes, highlighting the importance of membrane screening. This work did not aim to optimize the upstream feeds but rather it aimed to demonstrate the downstream

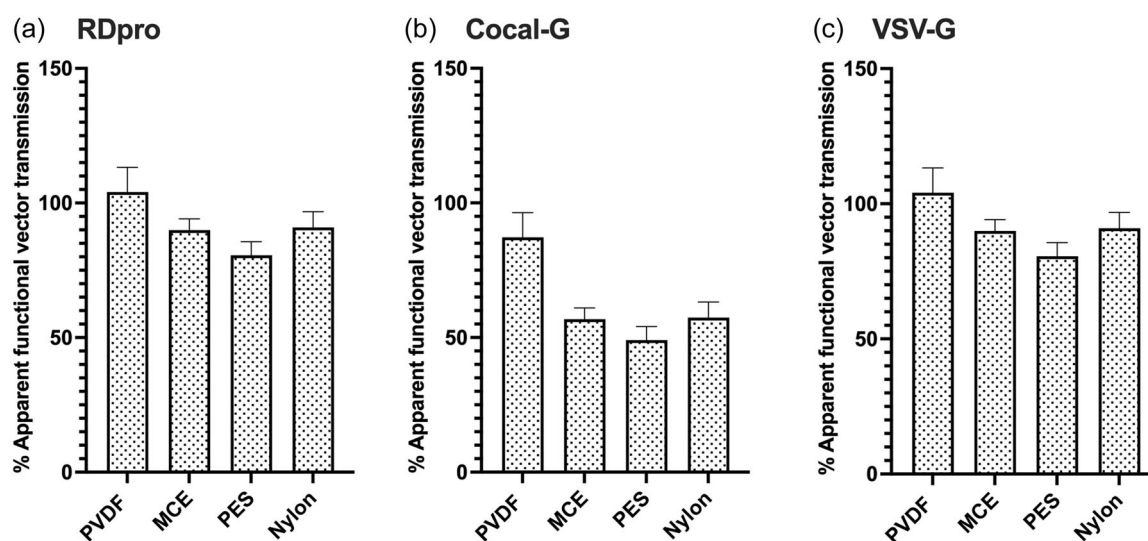


**FIGURE 3** Impact of membrane chemistry on the % apparent transmission of functional vector (i.e., vector in permeate ÷ vector in feed) × 100% after membrane clarification of transiently produced three-plasmid LVs with envelope protein: (a) VSV-G, (b) Cocal-G, and (c) RDpro. Thawed crude vector harvest was loaded on to 96-well plates with different membrane chemistries and filtered by vacuum at 500 mbar. Error bar is 1 SD based on N = 3 filtration wells.

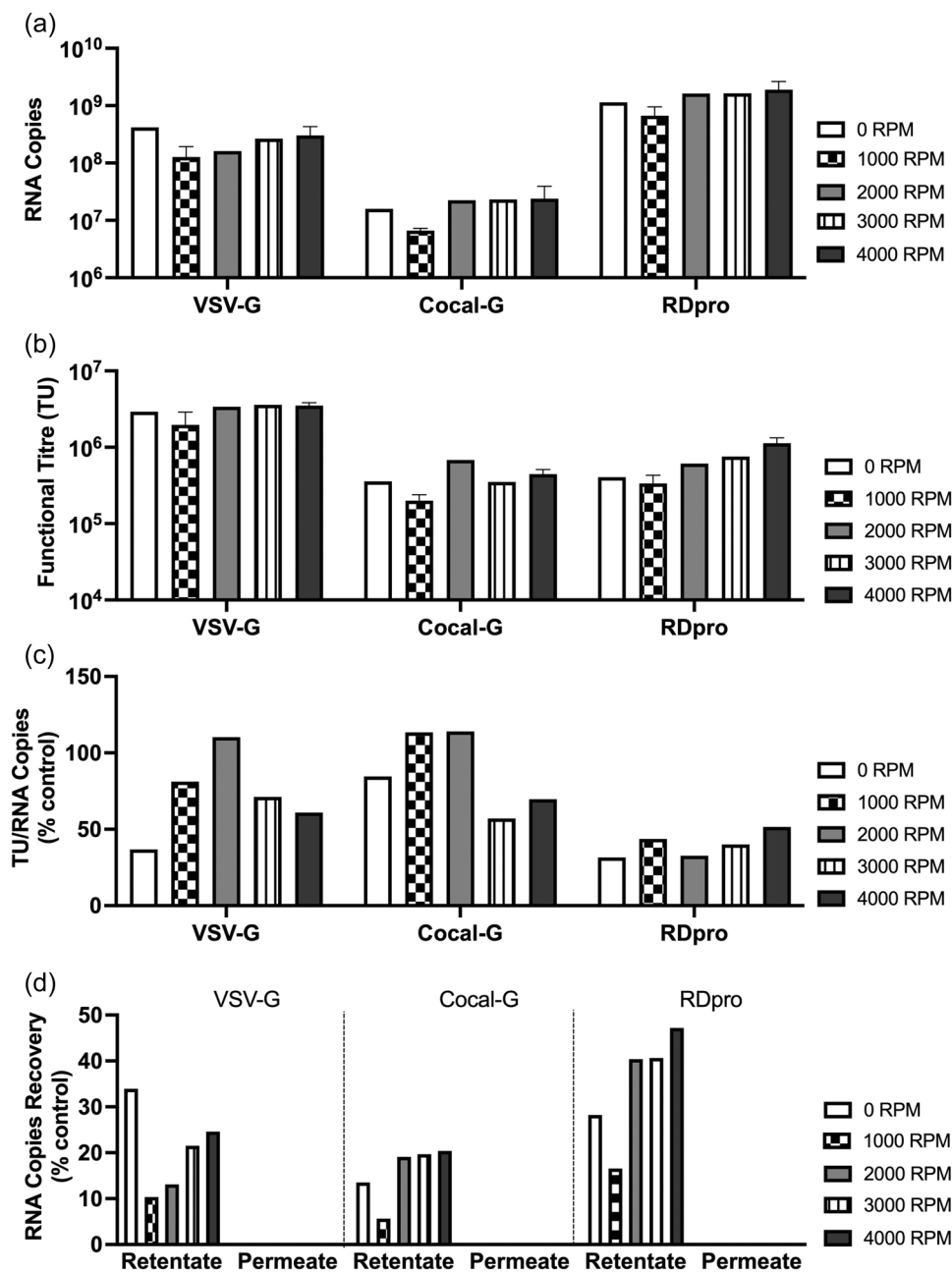


**FIGURE 4** Diafiltration studies of lentiviral vectors using the ultra scale-down membrane device showing in (a) total vector genome (RNA copies) and (b) total functional vector (TU) recovered from the USD-TFF operations; (c) %vector genome (RNA copies) by RNA reverse transcription polymerase chain reaction relative to control; and (d) %ratio of transducing units to RNA copies relative to control. Vector genome from the control for VSV-G, Cocal-G, and RDpro lentiviral vectors (LVs) are  $1.23\text{E} + 09$ ,  $1.18\text{E} + 08$ , and  $4.03\text{E} + 09$  RNA copies, respectively. Infectious titers from the control for VSV-G, Cocal-G, and RDpro LVs are  $2.35\text{E} + 07$ ,  $3.13\text{E} + 06$ , and  $4.65\text{E} + 06$  total transduction units, respectively. Viral vectors were transiently produced from the three-plasmid system. Vector samples were pumped through 500 kDa polyethersulfone filters in the USD membrane device at varying RPMs with equivalent shear rates of 0, 800, 2000, 4000, and  $5500\text{ s}^{-1}$ . Shear rate was at  $0\text{ s}^{-1}$  and membranes were not present in control experiments (i.e., samples simply flowed through the device).  $N = 3$  for 4000 RPM,  $N = 2$  for 1000 RPM,  $N = 1$  for all others. Error bars are 1 SD. TFF, tangential flow filtration; USD, ultra scale-down.

performance of these feeds as enabled by the ultra scale-down and high throughput methods as a screening tool. Furthermore, this study only focused on functional vector titers as a measure of filtrate quality. To help understand membrane and LV feed interaction, and therefore improve membrane process recoveries,

additional information on protein and DNA removal as well as fouling modes are needed. This is another subject of on-going work in our lab. Since batch-to-batch variation in LVs is common, designing a robust DSP will facilitate improved viral vector recoveries.

### 3.3 | Effect of shear during TFF operations

#### 3.3.1 | Ultra scale-down (USD) TFF mimic

An USD TFF mimic was used in this work to evaluate the impact of shear forces encountered during diafiltration of vector-containing media (i.e., crude harvests) of the various LV pseudotypes. To test if vector integrity is affected, RNA quantification was taken to evaluate total vector particles (Figure 4a) while a transduction assay was performed to quantify total functional vectors (Figure 4b) recovered from the USD-TFF device. These results show the combined impact of shear and membrane filter interaction with LVs. The data at 0 RPM illustrate the impact of membrane alone as there is no impact of shear at this condition. Overall, the data suggests that increasing shear rates from the lowest shear rate applied ( $\sim 800 \text{ s}^{-1}$  at 1000 RPM) during TFF-DF operation is necessary to recover more of the LV particles, including functional vectors. When data from LV production in literature was analyzed, it was observed that the equivalent shear rates in these LV studies are less than  $2000 \text{ s}^{-1}$ , and TFF field specialists have confirmed that some even run TFF operations at very slow flowrates corresponding to less than  $500 \text{ s}^{-1}$  (personal communication). The shear rates using the USD TFF-mimics in this work are more than twice as high as these shear rates currently used in LV production. During TFF operations, the shear across the membrane is necessary to maintain high permeate flux rates and to reduce, if not prevent, fouling of membranes. The shear rates are also linked to feed flowrates and therefore affect productivity of the manufacturing process. These current results indicate that there is scope in increasing LV recovery by optimizing the shear rates adopted during TFF operations for specific LV pseudotypes.

Additionally, there is a need to investigate membrane materials since the functional vectors and RNA copies from all the control runs (i.e., no membrane, no shear) are an order of magnitude higher than the vectors from USD diafiltration. These indicate that the effect of membranes on LV recovery is larger than the effect of shear. Figure 4c shows this for RNA copies, obtaining less than 50% of vector particles as %control. This figure further highlights the need to investigate membrane filter–LV interactions since no particles are detected in the permeates.

The ratio of transducing units relative to vector genomes acts as an estimate for vector integrity where decreasing ratio indicates loss of functional titers relative to RNA copies. Figure 4d compares TU/RNA copies of the TFF samples to non-sheared, nonfiltered control samples (i.e., as %control). For VSV-G and Cocal-G LVs, higher quality of particles can be achieved between  $800$  and  $2000 \text{ s}^{-1}$  (at  $1000$ – $2000$  rpm in the USD TFF) while this can be achieved at  $5000 \text{ s}^{-1}$  for RDpro LVs. Combined with the actual functional vectors in Figure 4b, these quality indicators in Figure 4c provide insights for the optimal shear rate for each LV pseudotype.

Separate larger scale studies, using commercial hollow fiber TFF systems, have demonstrated comparable results to the USD system where TFF runs at higher shear rates and relatively higher transmembrane pressure have improved LV recoveries (data not shown). This has demonstrated that insights gained from USD bioprocessing of LVs can be

utilized to scale up TFF processes. The results of these scale-down/scale-up studies are being prepared in a separate publication.

#### 3.3.2 | USD shear studies

Studying the effects of shear during TFF itself is complicated by the interaction of the membrane with the LVs which is already shown in Section 3.2 to potentially cause a reduction in functional vectors. To independently test the influence of process shear, the kompAs<sup>®</sup> ultra scale-down device (Rayat et al., 2016) was used to apply shear, with a spinning disc, on vector-containing media with different LVs. This device generates shear, at the tip of the disc, that mimic those encountered in industrial pumps and high-speed industrial disc stack centrifuges for solid-liquid separation (Nunes et al., 2023). Such magnitude of shear rates is typically higher than the shear rates experienced in TFF operations and ultracentrifuges. Results in Figure 5 demonstrate, for the first time, that

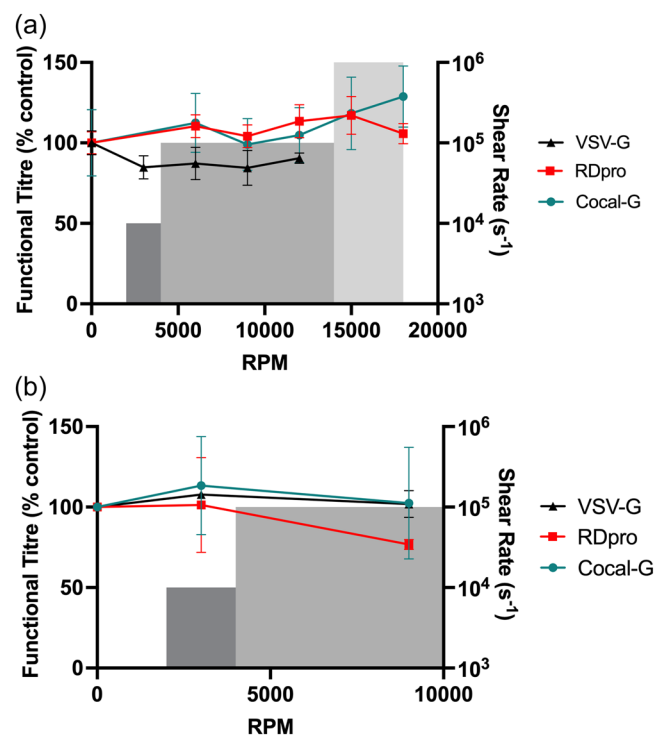


**FIGURE 5** USD shear study: relative transduction ability of viral vectors under increasing hydrodynamic shear rates for (a) three-plasmid system and (b) four-plasmid system in comparison to non-sheared control as measured by infectious titers assay. Shaded background represents magnitude of shear rates within the range of RPM in the USD device:  $10^4 \text{ s}^{-1}$  (dark gray)  $10^5 \text{ s}^{-1}$  (medium gray) and  $10^6 \text{ s}^{-1}$  (light gray). In (a), the non-sheared control titers for Cocal-G LV is  $8.76 \text{ E} + 04 \text{ TU mL}^{-1}$ , RDpro LV is  $3.41 \text{ E} + 05 \text{ TU mL}^{-1}$  and VSV-G LV is  $4.67 \text{ E} + 06 \text{ TU mL}^{-1}$  while in (b), titers for Cocal-G, RDpro and VSV-G LVs are  $6.36 \text{ E} + 06$ ,  $4.73 \text{ E} + 05$ , and  $1.99 \text{ E} + 06 \text{ TU mL}^{-1}$ , respectively. Error bars in (a) represent 1 SD for  $N = 3$  technical repeats. Error bars in (b) represent 1 SD for  $N = 2$  experiments, where for each experiment the reported titers is an average of three technical repeats. USD, ultra scale-down.

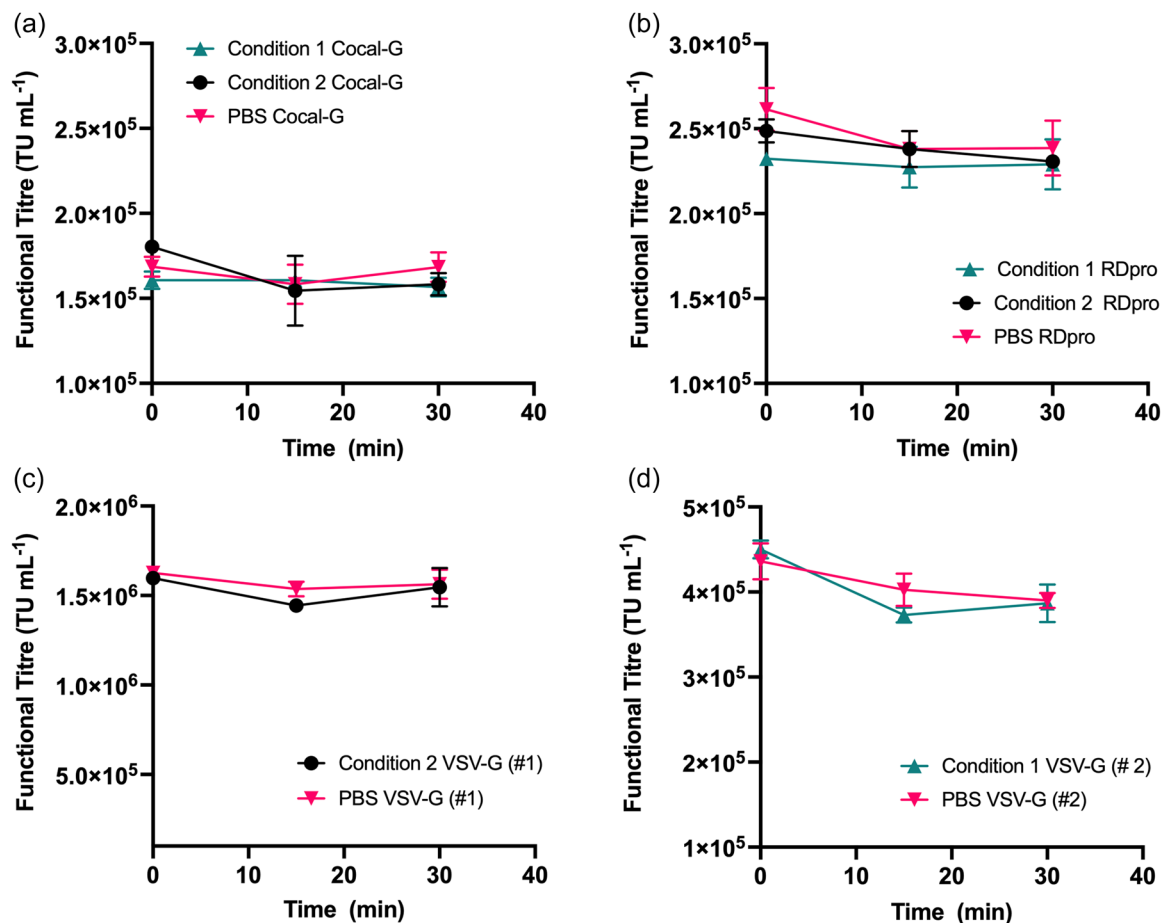


**FIGURE 6** Vector stability under varied buffer conditions over time for (a) Cocal-G, (b) RDpro, and (c) VSV-G Batch 1 Condition 2, (d) VSV-G Batch 2 Condition 1 compared with phosphate buffered saline controls. Conditions 1 and 2 are the optimum loading buffer conditions for the DEAE and Q monoliths, respectively, as shown in Table 2. Vector samples were transferred into binding buffer and incubated at room temperature. At the specified intervals, a sample of vector was diluted in complete media and assayed for infectious titers. Error bars based on 1 SD from  $N = 3$  monolith wells.

LVs are stable even when exposed to very high shear. The shear rates from the kompAs<sup>®</sup> device that was used in this study goes over  $10^5 \text{ s}^{-1}$  which is higher than the shear rates typically encountered in LV processing. In comparison, mAbs TFF (i.e., UF/DF) operate up to and around  $8000 \text{ s}^{-1}$  (Fernandez-Cerezo et al., 2020). A closer inspection of the yields in Figure 5a shows that for Cocal-G and RDpro enveloped LVs, the overall functional titers appears to increase with higher shear. However, VSV-G envelope protein has a mild decrease from initial to 3000 RPM, but titers from this point onwards is maintained. This may be due to VSV-G LVs being generated transiently, therefore demonstrating a more variable population which may be more susceptible to damage. As Cocal-G and RDpro were from clonal stable producer cell lines in this part of the study, these may be more robust. Likewise, free envelope proteins, or other inhibiting components, generated due to higher expression in transient generation compared to stable generation that are otherwise trapped in proteinaceous masses, may be liberated under shear. The LVs produced from the four-plasmid system also do not show any detrimental impact of very high shear rates, including VSV-G enveloped LVs (Figure 5b). Overall, these results indicate that LVs are generally not

sensitive to shear alone. The impact of shear is compounded by other factor interactions that are present in a unit operation (e.g., types of surfaces where the LVs encounter the high shear such as membranes and formulation buffer/media in TFF operations or tubing material during pump flow and fluid transfer). Buffer or media conditions may affect the stability of vectors and the fluid dynamics within a TFF system. Since the focus in this work was limited to study the impact of shear on the different LV pseudotypes, the same diafiltration media (DMEM) was useful for all LV materials to avoid the potential impact of, and factor-interaction contributed by, having a different buffer or media.

### 3.4 | Stability of LVs in chromatography buffers

#### 3.4.1 | Stability over time

During a Design of Experiment (DoE) study for binding and elution for QA and DEAE monolith chromatography (Perry, 2021), pH and NaCl concentration in 20 mM MOPS buffer was optimized across

pseudotyped LV groups. To test if the stability of the vector was impacted by buffer selection independent of the chromatography operation, an experiment evaluated the function of the vectors in a variety of buffers as determined by the earlier DoE study. In extension to this, a follow up experiment was generated testing impacts of elevated NaCl concentration more than typically used by AEX chromatography.

As shown in Figure 6, there is no overt difference in functional titers between vectors in binding buffers and in a generic PBS buffer. This is the case across all LV envelope proteins. There is minor decrease in functional titers over time compared to time point zero, but this decrease is minimal and is likely due to assay variation. Little difference is observed in Figure 7 between high and low NaCl concentration. Instead, zero NaCl conditions was linked to low functional vector titers which mean that some salt may be required to maintain vector function, either by stabilization of the vector particles and/or envelope by charge-based interactions or osmotic pressure. The relative resistance to high NaCl conditions does indicate some degree of stability over the time frame used in the study. Decreases in titers may be possible beyond this time period, however it is expected that in a typical bioprocess further processing would be considered and the vector may be diluted or buffer-exchanged. Ghosh et al. (2022) also demonstrated that LVs retain high recoveries even at high salt concentrations for certain chromatography conditions indicating the opportunity to design efficient LV processes.

### 3.4.2 | Comparison of monolith chromatography

Once stability of the lentiviral vectors was confirmed, the optimized binding and elution buffers were evaluated during QA monolith chromatography operations using clarified harvests. The chromatography operation using these optimized buffers were compared to base cell media DMEM to reflect vector loaded without any prior buffer exchanging. The composition of DMEM typically contains some salts, with NaCl at 110 mM, including other inorganic salts, and a pH range between 7.2 and 7.4, although this is likely lower with time in cell culture. Fresh DMEM was used here. Observations on vector yields in all tested buffer types (Figure 8(ii)) show that % recovery of functional vectors from the elution step was generally greater than 80% except for RDpro which was 54% for R2 (use of optimized buffers) and 67% for R1 (DMEM was used for loading). Optimized conditions (R2) outperformed DMEM (R1) in % recovery, although some Cocal-G vectors are present in the flowthrough fraction. No vectors were detected in the wash fraction across all conditions.

For total protein recovery, the majority was lost as flowthrough during the initial binding (Figure 8(ii)). Very little protein is present in the wash fraction across all samples. However, coelution of protein was observed in monolith operations using DMEM for loading the vectors. In optimized conditions, this range of recovery is 1%–6%, whereas for DMEM it is 7%–11%. There is an indication that mild

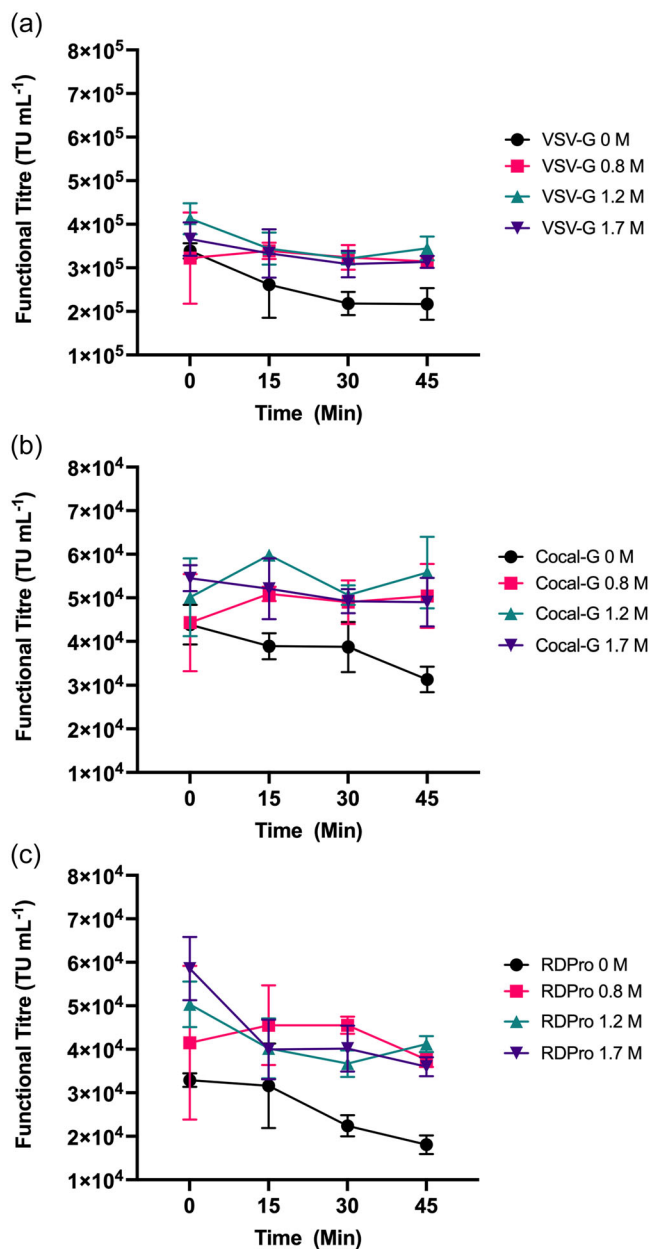


**FIGURE 7** Vector stability profile in elution buffer with increasing salt concentration showing functional titers of (a) VSV-G, (b) Cocal-G, and (c) RDpro enveloped lentiviral vectors. Buffer is 20 mM MOPS at pH 7.4 with NaCl at variable concentration as shown on data legends. Vectors were buffer exchanged prior into elution conditions. Every 15 min a sample of vector was diluted in complete media and used in a transduction assay to determine the infectious titers. Error bars are 1 SD based on  $N = 3$ .

improvements in optimized conditions prevented most protein from binding during loading. This may improve the binding capacity of the AEX media from lack of competition although this needs to be investigated.

Despite improvements in most metrics, DNA (Figure 8(iii)) was recovered at elution in all runs (>88%). The DNA concentration for eluted VSV-G and RDpro LVs was lower in the optimized loading

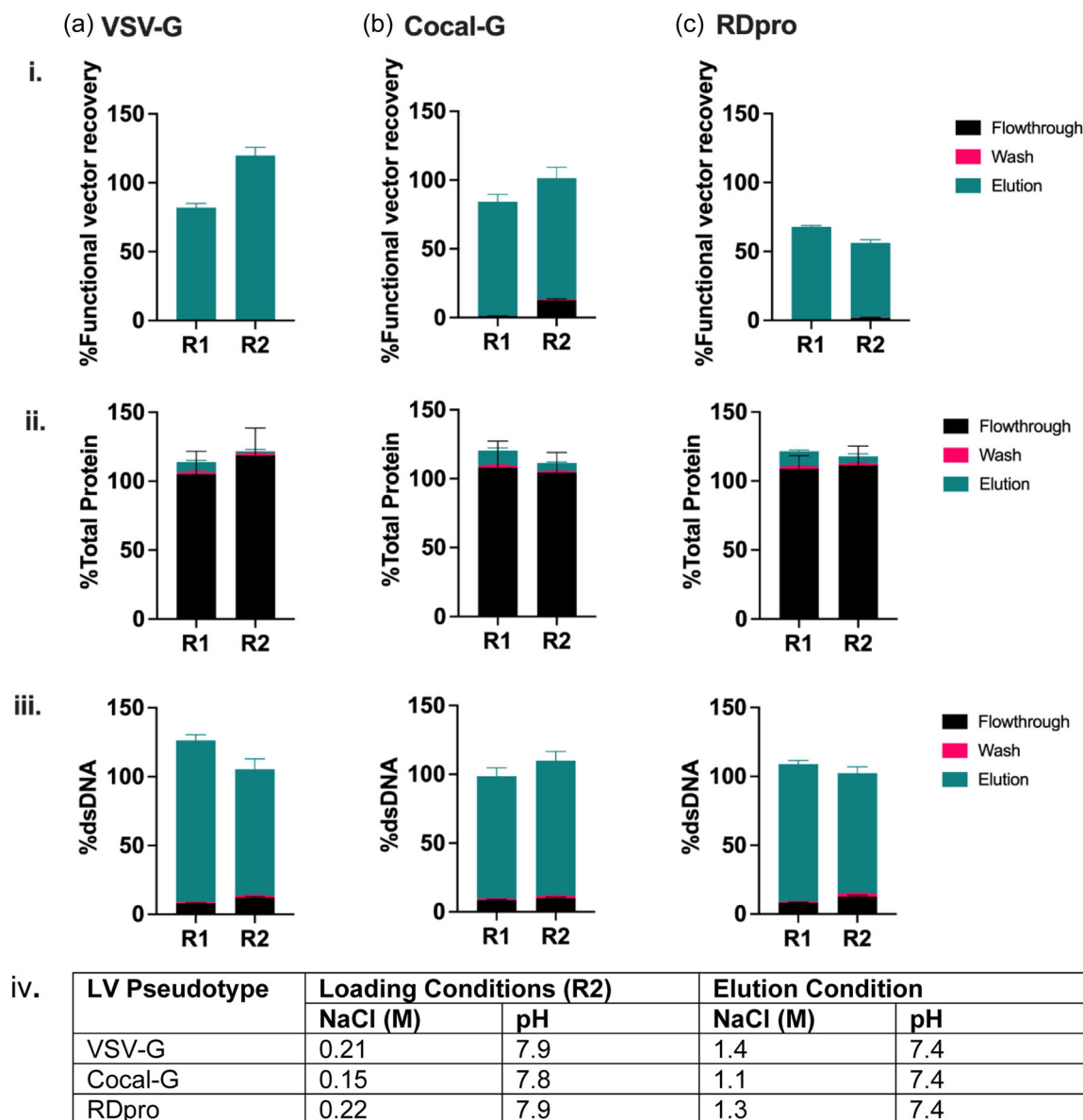


**FIGURE 8** Process responses using optimized and nonoptimized loading and elution conditions across (a) VSV-G, (b) Cocal-G, and (c) RDpro enveloped lentiviral vectors feeds showing: (i) % recovery of functional vector, (ii) total protein, and (iii) total DNA as cumulative fractions during processing. Vectors were transferred into DMEM (R1) or optimized binding buffer (R2, i.e., 20 mM MOPS in different salt conditions) before loading onto QA 96-well monolith column, washed and eluted in optimized elution buffer (20 mM MOPS with varying salt concentration). Vector, total protein and DNA was determined by transduction assay, Bradford and PicoGreen respectively. Error bars are 1 SD based on  $N = 3$ .

conditions, while Cocal-G vectors had higher DNA elution in optimized than DMEM. DNA was present in all flowthrough fractions, with higher DNA in flowthroughs in optimized loading conditions. As DNA appears to coelute at similar conditions as the vectors, the importance of minimizing DNA binding to the AEX media is essential, therefore efforts to prevent its binding is necessary. Salt gradient may reduce DNA during elution, although this may extend process times and potentially lose the vectors before collection since LVs do not correlate to UV traces in eluate. Endonucleases can be added before or after AEX although this may come at higher cost and further purification demand. Mixed mode chromatography may be beneficial, whereby size exclusion material prevents the vector

reaching the AEX core which otherwise depletes residual DNA. Here, it may be useful in further polishing of a diluted eluate, or before AEX entirely if properly sized considering the higher total protein concentration.

There is a loss of titers across elution as not all transducing units are accounted for. Numerous reasons can explain why some vectors were left bound on the monolith and did not elute. One reason is physical damage to the vector from bulk flow when immobilized to AEX media. In addition, due to their size, vectors are likely to bind at multiple locations of the AEX material and could bind too tightly. This may require even stronger elution conditions or prolonged residence time (i.e., incubation in the monolith wells), perhaps a lower vacuum

pressure could be used (e.g., 100 mbar). Further, the presence of some protein during elution has been observed to stabilize vector (Mekkaoui et al., 2018) and no such supplementation was used in these experiments. The impact of protein concentration and the physical binding to chromatographic stationary phases on vector stability was not investigated further but would be a worthy topic for future studies.

This monolith study relied on small scale vacuum plates for high throughput investigation. While suitable for screening of buffer composition, we acknowledge the benefit of investigating constant flow modalities of this unit operation. Likewise, the next step of this study would be to confirm at a larger different scale. This was not carried out due to limited feed material.

As the vectors were transiently generated, they are likely variable in quality due to differing transfection efficiencies of the producer cells. Therefore, their bind and elute conditions may naturally vary. Additional assays to quantify vectors would be beneficial, such as p24 ELISA, or western blot analysis which may inform on the components of the flowthrough or elution in addition to qPCR-based product enhanced reverse transcriptase assays (PERT) and electron microscopy for nonfunctional vector particles or degraded particles observation (Perry & Rayat, 2021).

## 4 | CONCLUSION

This work investigated bioprocessing conditions on the recovery of LVs and the impact of envelope protein choice on their success. This contributes to the improvement of these bioprocesses that will facilitate the efficient generation of vectors for advanced therapy purposes. We have demonstrated the effect of pump flow and manufacturing temperatures. For the specific vector samples used here, membrane filtration studies showed that PVDF and PES performed best and worst respectfully across all pseudotypes while Cocal-G enveloped vectors exhibited poor results compared to other enveloped LVs. Furthermore, in ultra scale-down studies we demonstrated resilience to shear across all vectors, while the TFF mimic indicated that higher shear improved recovery, although decreased ratio of functional titers to RNA was also observed, with adsorption onto the membrane a probable cause of vector loss. Demonstration of vector stability in optimized chromatography buffers and high salt conditions before a comparison in anion exchange monolith chromatography was shown. Vector recovery was improved over basic conditions for VSV-G and Cocal-G and enhanced total protein removal in flowthrough across all LV envelopes. While dsDNA remains a common impurity regardless of conditions applied. These results reinforce the need to experimentally test new LV products in terms of their robustness for manufacture. Scale-down manufacturing mimics enable such studies leading to greater understanding of LV processing, thus advancing their clinical applications. Biophysical characterization was not in scope. However, the process insights gained from ultra scale-down studies, such as those presented here, may reveal the potential route to mechanistic

understanding when done in tandem with biophysical characterization studies.

## AUTHOR CONTRIBUTIONS

**Christopher Perry:** Conceptualization, investigation, methodology, formal analysis, visualization, writing—original draft. **Noor Mujahid:** Conceptualization, investigation, validation, formal analysis, visualization, writing—original draft. **Yasu Takeuchi:** Conceptualization, supervision, data interpretation, writing—review and editing. **Andrea C. M. E. Rayat:** Conceptualization, funding acquisition, supervision, data interpretation, writing—review and editing.

## ACKNOWLEDGMENTS

This research was funded by the UKRI Engineering and Physical Sciences Research Council (EPSRC): for C.P. the Centre for Doctoral Training at the Department of Biochemical Engineering (EP/L01520X/1) and for N.M. the Doctoral Training Partnership at UCL (EP/N509577/1 and EP/T517793/1). C.P. was also supported by the National Institute for Biological Standards and Control (NIBSC)—Medicines and Healthcare Products Regulatory Agency (MHRA).

## DATA AVAILABILITY STATEMENT

The data that support the findings of this study are available from the corresponding author upon reasonable request.

## ORCID

Andrea C. M. E. Rayat  <http://orcid.org/0000-0003-4991-5300>

## REFERENCES

- Burns, J. C., Friedmann, T., Driever, W., Burrascano, M., & Yee, J. K. (1993). Vesicular stomatitis virus G glycoprotein pseudotyped retroviral vectors: Concentration to very high titer and efficient gene transfer into mammalian and nonmammalian cells. *Proceedings of the National Academy of Sciences of the United States of America*, 90(17), 8033–8037. <https://doi.org/10.1073/PNAS.90.17.8033>
- CGT Catapult. (2022). *Cell and gene therapy catapult UK ATMP clinical trials Report 2022*.
- Chen, Y. H., Keiser, M. S., & Davidson, B. L. (2018). Viral vectors for gene transfer. *Current Protocols in Mouse Biology*, 8(4), e58. <https://doi.org/10.1002/cpmo.58>
- Comisel, R. M., Kara, B., Fiesser, F. H., & Farid, S. S. (2021). Lentiviral vector bioprocess economics for cell and gene therapy commercialization. *Biochemical Engineering Journal*, 167, 107868. <https://doi.org/10.1016/J.BEJ.2020.107868>
- Cronin, J., Zhang, X.-Y., & Reiser, J. (2005). Altering the tropism of lentiviral vectors through pseudotyping. *Current Gene Therapy*, 5(4), 387–398. <https://doi.org/10.2174/1566523054546224>
- Dalgleish, A. G., Beverley, P. C. L., Clapham, P. R., Crawford, D. H., Greaves, M. F., & Weiss, R. A. (1984). The CD4 (T4) antigen is an essential component of the receptor for the AIDS retrovirus. *Nature*, 312(5996), 763–767. <https://doi.org/10.1038/312763A0>
- Dautzenberg, I., Rabelink, M., & Hoeben, R. C. (2021). The stability of envelope-pseudotyped lentiviral vectors. *Gene Therapy*, 28, 89–104. <https://doi.org/10.1038/s41434-020-00193-y>
- Dull, T., Zufferey, R., Kelly, M., Mandel, R. J., Nguyen, M., Trono, D., & Naldini, L. (1998). A third-generation lentivirus vector with a conditional packaging system. *Journal of Virology*, 72(11), 8463–8471.

- Durand, S., & Cimarelli, A. (2011). The inside out of lentiviral vectors. *Viruses*, 3, 132–159. <https://doi.org/10.3390/v3020132>
- Fernandez-Cerezo, L., Rayat, A. C. M. E., Chatel, A., Pollard, J. M., Lye, G. J., & Hoare, M. (2019). An ultra scale-down method to investigate monoclonal antibody processing during tangential flow filtration using ultrafiltration membranes. *Biotechnology and Bioengineering*, 116, 581–590.
- Fernandez-Cerezo, L., Rayat, A. C. M. E., Chatel, A., Pollard, J. M., Lye, G. J., & Hoare, M. (2020). The prediction of the operating conditions on the permeate flux and on protein aggregation during membrane processing of monoclonal antibodies. *Journal of Membrane Science*, 596, 117606.
- Fox, T., Bueren, J., Candotti, F., Fischer, A., Aiuti, A., Lankester, A., Agora, I., & Booth, C. (2023). Access to gene therapy for rare diseases when commercialization is not fit for purpose. *Nature Medicine*, 29, 518–519. <https://doi.org/10.1038/s41591-023-02208-8>
- Ghani, K., Wang, X., De Campos-Lima, P. O., Olszewska, M., Kamen, A., Rivière, I., & Caruso, M. (2009). Efficient human hematopoietic cell transduction using RD114- and GALV-pseudotyped retroviral vectors produced in suspension and serum-free media. *Human Gene Therapy*, 20(9), 966–974. <https://doi.org/10.1089/HUM.2009.001/ASSET/IMAGES/LARGE/FIG-6.JPEG>
- Ghosh, R., Koley, S., Gopal, S., Rodrigues, A. L., Dordick, J. S., & Cramer, S. M. (2022). Evaluation of lentiviral vector stability and development of ion exchange purification processes. *Biotechnology Progress*, 38(6), e3286. <https://doi.org/10.1002/btpr.3286>
- Hoffmann, M., Wu, Y. J., Gerber, M., Berger-Rentsch, M., Heimrich, B., Schwemmler, M., & Zimmer, G. (2010). Fusion-active glycoprotein G mediates the cytotoxicity of vesicular stomatitis virus M mutants lacking host shut-off activity. *Journal of General Virology*, 91(11), 2782–2793. <https://doi.org/10.1099/VIR.0.023978-0/CITE/REFWORKS>
- Huisman, I. H., Prádanos, P., & Hernández, A. (2000). The effect of protein-protein and protein-membrane interactions on membrane fouling in ultrafiltration. *Journal of Membrane Science*, 179(1–2), 79–90. [https://doi.org/10.1016/S0376-7388\(00\)00501-9](https://doi.org/10.1016/S0376-7388(00)00501-9)
- Humbert, O., Gisch, D. W., Wohlfahrt, M. E., Adams, A. B., Greenberg, P. D., Schmitt, T. M., Trobridge, G. D., & Kiem, H. P. (2016). Development of third-generation cocl envelope producer cell lines for robust lentiviral gene transfer into hematopoietic stem cells and t-cells. *Molecular Therapy*, 24(7), 1237–1246. <https://doi.org/10.1038/MT.2016.70>
- Kalidasan, V., Ng, W. H., Ishola, O. A., Ravichantar, N., Tan, J. J., & Das, K. T. (2021). A guide in lentiviral vector production for hard-to-transfect cells, using cardiac-derived c-kit expressing cells as a model system. *Scientific Reports*, 11, 19265. <https://doi.org/10.1038/s41598-021-98657-7>
- Kim, S. H., & Lim, K. I. (2017). Stability of retroviral vectors against ultracentrifugation is determined by the viral internal core and envelope proteins used for pseudotyping. *Molecules and Cells*, 40(5), 339–345. <https://doi.org/10.14348/molcells.2017.0043>
- McCarron, A., Donnelley, M., McIntyre, C., & Parsons, D. (2016). Challenges of up-scaling lentivirus production and processing. *Journal of Biotechnology*, 240, 23–30. <https://doi.org/10.1016/j.jbiotec.2016.10.016>
- Mekkaoui, L., Parekh, F., Kotsopoulou, E., Darling, D., Dickson, G., Cheung, G. W., Chan, L., MacLellan-Gibson, K., Mattiuzzo, G., Farzaneh, F., Takeuchi, Yasuhiro., & Pule, M. (2018). Lentiviral vector purification using genetically encoded biotin mimic in packaging cell. *Molecular Therapy - Methods & Clinical Development*, 11, 155–165. <https://doi.org/10.1016/j.omtm.2018.10.008>
- Milone, M. C., & O'Doherty, U. (2018). Clinical use of lentiviral vectors. *Leukemia*, 32(7), 1529–1541. <https://doi.org/10.1038/s41375-018-0106-0>
- Moreira, A. S., Cavaco, D. G., Faria, T. Q., Alves, P. M., Carrondo, M. J. T., & Peixoto, C. (2020). Advances in lentivirus purification. *Biotechnology Journal*, 16(1), 2000019. <https://doi.org/10.1002/biot.202000019>
- Müller, S., Bexte, T., Gebel, V., Kalensee, F., Stolzenberg, E., Hartmann, J., Koehl, U., Schambach, A., Wels, W. S., Modlich, U., & Ullrich, E. (2020). High cytotoxic efficiency of lentivirally and alpharetrovirally engineered CD19-specific chimeric antigen receptor natural killer cells against acute lymphoblastic leukemia. *Frontiers in Immunology*, 10, 3123. <https://doi.org/10.3389/FIMMU.2019.03123/BIBTEX>
- Munis, A. M., Tijani, M., Hassall, M., Mattiuzzo, G., Collins, M. K., & Takeuchi, Y. (2018). Characterization of antibody interactions with the G protein of vesicular stomatitis virus Indiana strain and other vesiculovirus G proteins. *Journal of Virology*, 92(23), e00900-18. <https://doi.org/10.1128/JVI.00900-18>
- Naldini, L., Blömer, U., Galloway, P., Ory, D., Mulligan, R., Gage, F. H., Verma, I. M., & Trono, D. (1996). In vivo gene delivery and stable transduction of nondividing cells by a lentiviral vector. *Science*, 272(5259), 263–267. <https://doi.org/10.1126/science.272.5259.263>
- Nunes, S. L. V., Mannall, G. J., & Rayat, A. C. M. E. (2023). Integrated ultra scale-down and multivariate analysis of flocculation and centrifugation for enhanced primary recovery. *Food and Bioprocess Processing*, 139, 61–74. <https://doi.org/10.1016/j.fbp.2023.02.008>
- Perry, C. (2021). *Lentiviral vector stability and process purification based on modifications to the viral envelope* [Doctoral thesis (Eng.D)]. UCL University College London.
- Perry, C., & Rayat, A. C. M. E. (2021). Lentiviral vector bioprocessing. *Viruses*, 13, 268. <https://doi.org/10.3390/v13020268>
- Rayat, A. C., Chatel, A., Hoare, M., & Lye, G. J. (2016). Ultra scale-down approaches to enhance the creation of bioprocesses at scale: Impacts of process shear stress and early recovery stages. *Current Opinion in Chemical Engineering*, 14, 150–157. <https://doi.org/10.1016/j.coche.2016.09.012>
- Ruscic, J., Perry, C., Mukhopadhyay, T., Takeuchi, Y., & Bracewell, D. G. (2019). Lentiviral vector purification using nanofiber ion-exchange chromatography. *Molecular Therapy—Methods & Clinical Development*, 15(December), 52–62. <https://doi.org/10.1016/j.omtm.2019.08.007>
- Sakuma, T., Barry, M. A., & Ikeda, Y. (2012). Lentiviral vectors: Basic to translational. *Biochemical Journal*, 443(3), 603–618. <https://doi.org/10.1042/BJ20120146>
- Sanber, K. S., Knight, S. B., Stephen, S. L., Bailey, R., Escors, D., Minshull, J., Santilli, G., Thrasher, A. J., Collins, M. K., & Takeuchi, Y. (2015). Construction of stable packaging cell lines for clinical lentiviral vector production. *Scientific Reports*, 5, 9021. <https://doi.org/10.1038/srep09021>
- Takeuchi, Y., Cosset, F. L., Lachmann, P. J., Okada, H., Weiss, R. A., & Collins, M. K. (1994). Type C retrovirus inactivation by human complement is determined by both the viral genome and the producer cell. *Journal of Virology*, 68(12), 8001–8007. <https://doi.org/10.1128/JVI.68.12.8001-8007.1994>
- Tijani, M., Munis, A. M., Perry, C., Sanber, K., Ferrareso, M., Mukhopadhyay, T., Themis, M., Nisoli, I., Mattiuzzo, G., Collins, M. K., & Takeuchi, Y. (2018). Lentivector producer cell lines with stably expressed vesiculovirus envelopes. *Molecular Therapy—Methods & Clinical Development*, 10(September), 303–312. <https://doi.org/10.1016/j.omtm.2018.07.013>
- Titchener-Hooker, N. J., Dunnill, P., & Hoare, M. (2008). Micro biochemical engineering to accelerate the design of industrial-scale downstream processes for biopharmaceutical proteins. *Biotechnology and Bioengineering*, 100(3), 473–487. <https://doi.org/10.1002/bit.21788>



- United States of America FDA. (2022). *Approved cellular and gene therapy products*. Retrieved April 3, 2023 from: <https://www.fda.gov/vaccines-blood-biologics/cellular-gene-therapy-products/approved-cellular-and-gene-therapy-products>
- Zydney, A. L. (2021). New developments in membranes for bioprocessing—A review. *Journal of Membrane Science*, 620(October), 118804. <https://doi.org/10.1016/j.memsci.2020.118804>

**How to cite this article:** Perry, C., Mujahid, N., Takeuchi, Y., & Rayat, A. C. M. E. (2023). Insights into product and process related challenges of lentiviral vector bioprocessing. *Biotechnology and Bioengineering*, 1–16. <https://doi.org/10.1002/bit.28498>